



Seismic landslides hazard zoning based on the modified Newmark model: a case study from the Lushan earthquake, China

K. P. Jin¹ · L. K. Yao² · Q. G. Cheng³ · A. G. Xing¹

Received: 21 January 2019 / Accepted: 13 August 2019 / Published online: 17 August 2019
© Springer Nature B.V. 2019

Abstract

Seismically triggered landslides can cause great damage to the road construction in mountainous areas. The permanent displacement analysis based on Newmark sliding-block model can evaluate risk of these landslides from the perspective of deformation damage and overall failure probability of slopes. However, the sliding-block model does not consider the attenuation effect of the shear strength on the sliding surface during earthquake, causing the calculated value of Jibson method to be less than the actual value. Therefore, the Newmark model was modified by adding attenuation coefficients to the effective internal friction angle and the effective cohesion of geologic units. The landslide areal density was proposed for hazard zoning with the Wenchuan earthquake data. The results showed that the predicted values agreed well with the real distribution of the landslides triggered by the Lushan earthquake. The proposed hazard zoning method in this paper can predict the severity of seismic landslides in consideration of the environmental changes in mountainous regions after the earthquake and provide support for the site selection in highly seismic areas.

Keywords Seismically triggered landslides · Modified Newmark model · Landslide areal density · Hazard zoning method

1 Introduction

Co-seismic landslide is one of the most destructive hazards associated with earthquake (Yin et al. 2009; Gorum et al. 2011; Xu et al. 2014). The indirect damage caused by co-seismic landslides is far greater than the direct effect of earthquake itself (Rodriguez et al.

✉ A. G. Xing
xingaiguo@sjtu.edu.cn

¹ State Key Laboratory of Ocean Engineering, Shanghai Jiao Tong University, Shanghai 200240, People's Republic of China

² College of Civil Engineering, Southwest Jiaotong University, Chengdu 610031, People's Republic of China

³ Department of Geological Engineering, Southwest Jiaotong University, Chengdu 610031, People's Republic of China

1999; Keefer 2000; Ling et al. 2001, 2005; Huang and Li 2008; Duan et al. 2015). Therefore, estimating where and in what shaking conditions earthquakes are likely to trigger landslides is a key element in selecting the location of roads and towns (Wilson and Keefer 1985; Ambraseys and Menu 1988; Keefer and Wilson 1989; Wieczorek et al. 1993; Jibson and Keefer 1993; Ambraseys and Srbulov 1994; Khazai and Sitar 2000; Jibson et al. 2000; Romeo 2000; Decanini and Fabrizio 2001; Lveda et al. 2005; Kokusho and Ishizawa 2006; Bray and Travarasou 2007; Kokusho et al. 2009; Rodríguez-Peces et al. 2014; Huang and Xiong 2017; Huang et al. 2018). Newmark (1965) proposed the landslide model by modeling the landslide as a rigid block with friction that slides on an inclined plane, and the block will begin to slide against the friction of the sliding surface when the seismic intensity exceeds the seismic strength of the slope. Newmark displacement analysis requires two types of data: (1) the critical acceleration (a_c) of the slope, which is simply the base acceleration required to overcome shear resistance and initiate sliding; (2) the earthquake acceleration time history, which represents earthquake action. Since the earthquake acceleration time history can only be obtained after the earthquake, the Newmark model cannot be used for the prediction of landslides.

In the past 30 years, researchers used peak acceleration (*PGA*) and other parameters to replace the earthquake acceleration time history data in the Newmark model and established a series of regression equations to predict the Newmark displacements of the slope (Ambraseys and Menu 1988; Jibson 1993; Milesa and Ho 1999; Al-Homoud and Tahtamoni 2000; Romeo 2000; Shang and Lee 2011; Rajabi et al. 2011; Lee et al. 2012; Ma and Xu 2018). The relation curve with the critical acceleration ratio (a_c/a_{\max}) and the permanent displacement (D_N) as the independent variable and corresponding variables, respectively, is called the Jibson permanent displacement method. Since the peak acceleration of the earthquake can be determined by using the national zonation map of ground-motion peak acceleration. The critical acceleration is an inherent attribute of the slope. The Jibson method is practically applicable to the prediction of the permanent displacement of seismically triggered landslides. Recently, the Jibson method has been used internationally and has received recognition. For example, Chen et al. (2011) used the Jibson method to carry out mapping of earthquake-triggered landslides in the Yingxiu area.

However, the accuracy of the Jibson displacement prediction method has not been examined. Through analyzing the Newmark sliding-block model, we found that this model ignores the attenuation effect of the shear strength on the sliding surface during an earthquake, resulting in the calculated value of the Jibson method being smaller than the actual earthquake value. This inference was verified by real seismic data from the Wenchuan earthquake. Therefore, Jibson method was modified by adding attenuation coefficients to the shear strength in this paper.

Ultimately, a hazard zoning method based on the modified Jibson method was established to map the spatial distribution of landslides by referring to the rock failure model (Jaeger and Cook 1969). The relevant data of the Wenchuan earthquake were used to establish the hazard zoning method, and the correctness of the zoning method was tested by the seismic data of the Lushan earthquake.

2 Newmark model theory

2.1 Newmark sliding-block model

The potential landslide is modeled as a block resting on a plane inclined at an angle (α) from the horizontal (Newmark 1965). The block has a base acceleration required to overcome and initiate sliding, called the critical acceleration (a_c). The model calculates the permanent displacement of the block as it is subjected to a base acceleration (a), which representing the earthquake shaking (Fig. 1).

The Newmark displacement can be calculated by integrating the seismic acceleration-time history beyond the critical acceleration for twice (Fig. 2), and the equation is expressed as

$$D_N = \iint_t (a(t) - a_c) dt dt \tag{1}$$

where D_N is the Newmark permanent displacement, and $a(t)$ is the acceleration time history.

Newmark (1965) defines the critical acceleration of the block as a parameter containing the static factor of safety and slope geometry expressed as

$$a_c = (F_s - 1)g \sin \theta \tag{2}$$

where a_c is the critical acceleration; g is the acceleration due to Earth’s gravity; F_s is the static factor of safety; θ is the angle from the horizontal that the center of the potential slide block first moves, and it can be generally approximated as the slope angle.

The static factor of safety (F_s) in this condition is expressed as

$$F_s = \frac{(c')}{\gamma t \sin \alpha} + \frac{\tan(\varphi')}{\tan \alpha} - \frac{m\gamma_w \tan(\varphi')}{\gamma \tan \alpha} \tag{3}$$

where φ' is the effective friction angle; c' is the effective cohesion; α is the slope angle; γ is the material unit weight; γ_w is the unit weight of water; t is the slope-normal thickness of the failure slab; and m is the proportion of the saturated slab thickness in the slope. The

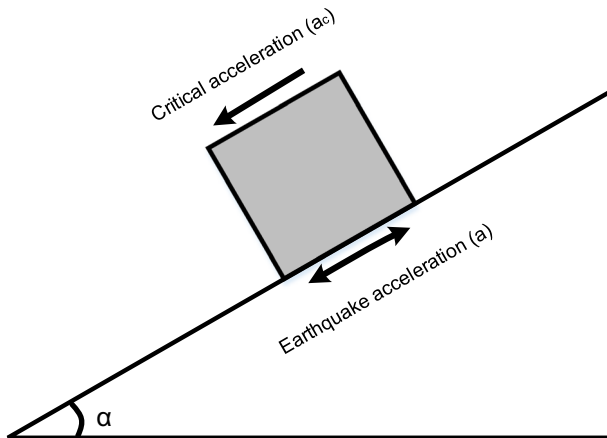
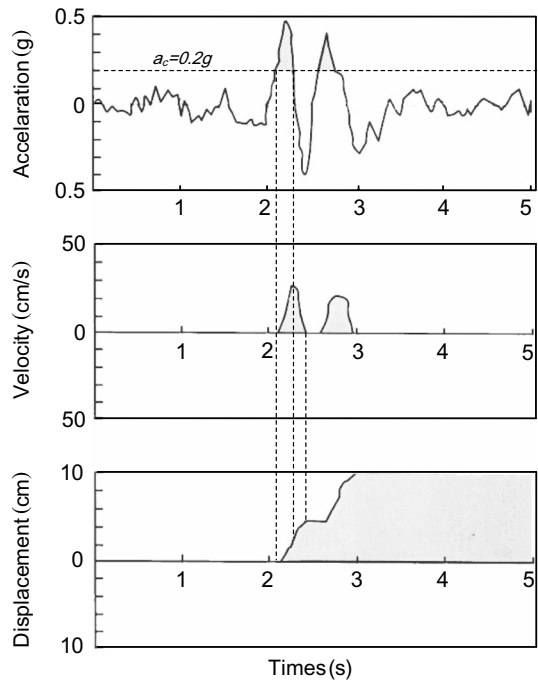


Fig. 1 Sliding-block model of Newmark analysis

Fig. 2 Demonstration of the Newmark-analysis algorithm. (a) Earthquake acceleration-time history with critical acceleration (horizontal dashed line) of 0.20 g superimposed. (b) Velocity of landslide block versus time. (c) Displacement of landslide block versus time



first term on the left side represents the cohesive component of the strength, the second term accounts for the frictional component, and the third term represents the reduction in frictional strength due to pore pressure.

The Newmark model cannot be used for predicting the permanent displacement, because the acceleration time history ($a_{(t)}$ in Eq. 1) can only be obtained using the seismological station after the earthquake.

2.2 Jibson method of permanent displacement prediction

Jibson (1993) used the peak ground acceleration (PGA) and other parameters that can be obtained before the earthquake to establish a new predicting method for the permanent displacement. In 2007, Jibson collected 2270 strong vibration records from 30 earthquakes around the world and re-established four regression equations based on the parameters of Arias intensity, critical acceleration, and critical acceleration ratio. Among these displacement prediction equations, the equation (Jibson 2007) with the critical acceleration ratio (a_c/a_{\max}) as the parameter has the best fit. It is expressed as:

$$\log D_N = 0.215 + \log \left[\left(1 - \frac{a_c}{a_{\max}} \right)^{2.341} \left(\frac{a_c}{a_{\max}} \right)^{-1.438} \right] \quad (4)$$

where a_{\max} is the peak ground acceleration, and a_c is the critical acceleration of the slope.

2.3 Theoretical defect of the Newmark sliding-block model

The Newmark model assumes that the critical acceleration of the block remains unchanged during the process of an earthquake, which ignores the dynamic attenuation of the shear strength on the sliding surface and causes the predicted value of the Jibson method to be smaller than the displacement caused by an actual earthquake. In fact, under a static load, the static cohesion and internal friction angle are taken as the shear strength parameters of the slope. However, under the dynamic load, the dynamic cohesion and internal friction angle should be taken as the shear strength parameters of the slope.

3 Modification of the Jibson method

The dynamic cohesion and internal friction angle (characterized by multiplying the static cohesion and internal friction angle by their respective attenuation coefficients) were used to calculate the critical acceleration under the dynamic load. In this way, the Newmark model was modified to improve the prediction accuracy of the Jibson method.

In this study, we mainly focus on the stability of highway slope in the Wenchuan earthquake. According to the field investigation, it was found that the highway slope is soil–rock medium, and the ratio of soil to rock is approximately 7:3. Therefore, we focused on the soil–rock medium (the ratio of soil to rock is 7:3) in this project. Also, the dynamic triaxial test results show that the attenuation coefficients of cohesion and internal friction angle of specimens with different soil–rock ratios vary from 0.55 to 0.7 and from 0.75 to 0.93, respectively (Wang et al. 2012). Since the highway slope is soil–rock medium and the ratio of soil to rock is approximately 7:3, thus, we determined that the attenuation coefficients of the cohesion and internal friction angle are 0.6 and 0.85, respectively. In order to improve the applicability of this method, further research will be conducted on the attenuation coefficients for a different soil and rock in the future.

Based on the analysis above, two attenuation coefficients were added into Eq. 3 to modify the static factor of safety in the Newmark model and expressed as

$$F_s = \frac{(0.6c')}{\gamma t \sin a} + \frac{\tan(0.85\phi')}{\tan a} - \frac{m\gamma_w \tan(0.85\phi')}{\gamma \tan a} \tag{5}$$

Result showed that the critical acceleration (a_c) is 0.7 times the previous one after taking the modified F_s into Eq. 2, and the modified equation of the Jibson method was proposed and expressed as

$$\log D_N = 0.215 + \log \left[\left(1 - \frac{0.7a_c}{a_{\max}} \right)^{2.341} \left(\frac{0.7a_c}{a_{\max}} \right)^{-1.438} \right] \tag{6}$$

The attenuation coefficients can be adjusted appropriately for areas with less seismic intensity.

Compared with the original model, the modified Jibson model considers the attenuation of shear strength of rock and soil under earthquakes and introduces attenuation coefficient. It perfects the Newmark model in terms of its mechanics.

4 Verification of modification effect using real seismic data

4.1 Data

The Wenchuan earthquake is one of the most devastating earthquakes recorded in the era of modern instrumentation, and it provides special conditions for testing the accuracy of the modified Jibson method. The process of the verification requires two aspects of data: (1) the real displacements (D_N) of slopes and (2) the a_c and PGA of slopes used for calculating the predicted displacements. Exactly, the Wenchuan earthquake provides special conditions for studying the Jibson method. The survey samples are mainly from the slopes (containing D_N , a_c , and PGA) along the roads in seismic areas, and the distribution of these slopes is shown in Fig. 3. The displacement of each slope was acquired by manual field measurement (Figs. 4 and 5). The critical acceleration of each slope was calculated through the slope parameters, and the PGA of each slope was obtained using the ground-motion attenuation model with the east–west acceleration time history recorded by the Wolong station during the Wenchuan earthquake (Cui et al. 2011). The information of D_N , a_c , and PGA is listed in Table 1.

4.2 Processing

In order to test the accuracy of the modified Jibson method (Fig. 6), the measured displacements of the slopes were put in the same coordinate axis with the prediction curves of the traditional Jibson method and the modified Jibson method. It was concluded that the modified equation agreed better with the measured value than the traditional equation in the

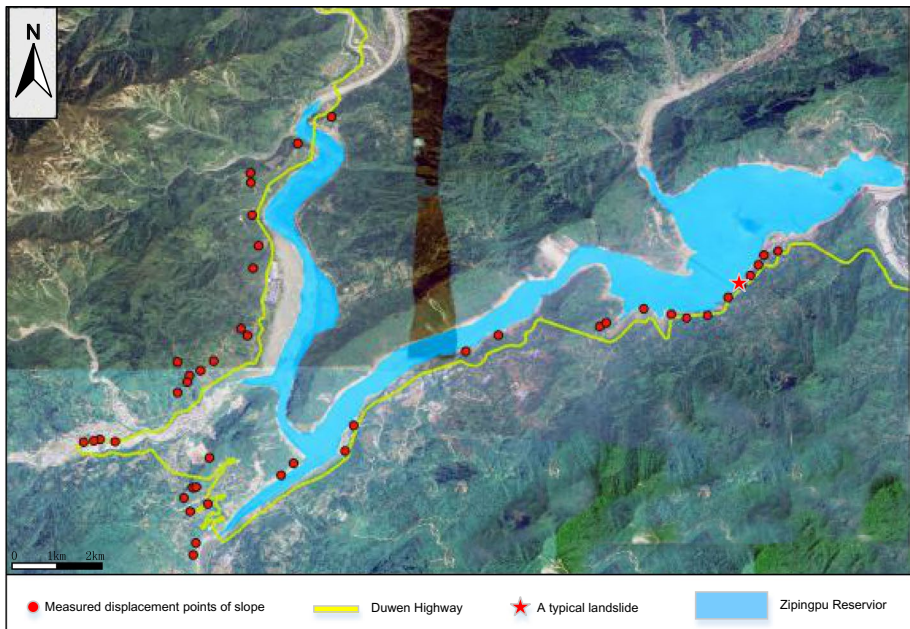


Fig. 3 Distribution of displacement collection points



Fig. 4 A typical landslide along the highway

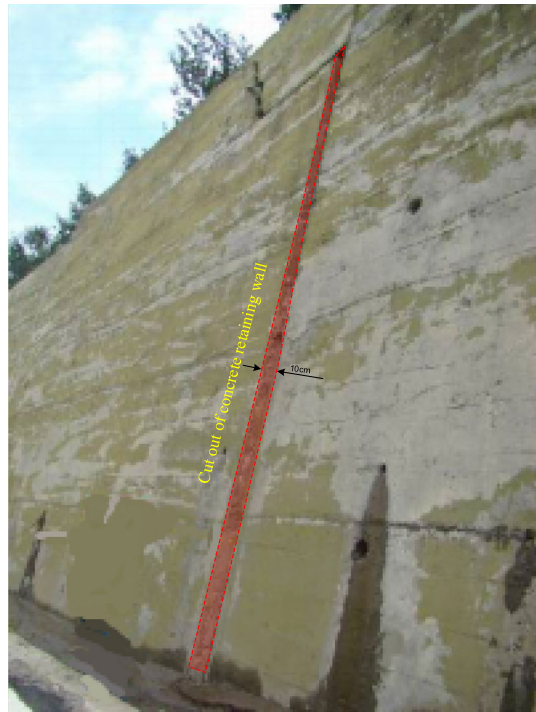
region with large seismic intensities (Fig. 6). However, the modified displacement value showed a larger trend than the measured value in the region with low seismic intensities. It can be explained that the attenuation coefficients of the internal friction angle and the cohesion force were set to be the fixed values in Eq. 6 for regions with large earthquake intensities, which means the attenuation effect was considered too strong for regions with low seismic intensities. Obviously, landslides triggered by strong earthquakes are the focus of our attention. In summary, the accuracy of the modified Jibson method was superior to that of the traditional method in regions with large earthquake intensities.

5 Hazard zoning for seismically triggered landslides based on a modified Jibson method

5.1 Relationship between Newmark displacement and areal density of landslides

Jibson used the Weibull curve to fit two parameters (Newmark permanent displacement and the probability of slope failure) with the data of 1994 Northridge earthquake and obtained the equation for the probability of slope failure (Jibson 2000). However, the areal density of landslides (the proportion of landslide area per square kilometer) can be

Fig. 5 Slippage from the concrete retaining wall's bottom



more intuitive than the probability of slope failure for seismic landslides. Therefore, the Weibull curve was used to fit the areal density of landslides and Newmark permanent displacements. Eventually, an equation for predicting the areal density of landslides was established.

The Wenchuan earthquake (magnitude 8.0) presents all of the data required for detailed regional analyses. Firstly, the northern part of the area from Maoxian to Beichuan County was chosen as the study area (Fig. 7). This area contains seismic intensity zones of IX, X, and XI. Moreover, the lithology is diverse, which facilitates the collection of representative permanent displacements and the areal density of landslides. Regions with slopes below 10° do not have the topographical conditions to trigger landslides and have been removed from the study area. Secondly, ArcGIS was used to collect the real areal density of earthquake-triggered landslides in the study area. Based on the collection of geological, topographical information (Wang et al. 2013), and *PGA* information in the study area, the modified Jibson method was used to calculate the slope permanent displacements. Two sets of data (areal density of landslides and permanent displacements) were projected to the same layer in ArcGIS, which facilitated their corresponding collection (Fig. 8). Since the permanent displacements calculated by the modified Jibson method are discrete values, ten sets of data were obtained. The average areal density of landslides corresponding to each set of displacement values was counted, respectively, and two sets of data were shown in Table 2.

The Weibull curve was used to fit two sets of data, and the relationship curve is shown in Fig. 9. The formula is as follows:

$$p = 0.301(1 - \exp(-0.00018D_N^{2.56})) R^2 = 0.98 \quad (7)$$

Table 1 Data of slope displacement acquisition points

| Nos. | Latitude (N) | Longitude (E) | DN (cm) | AC (g) | Calculated PGA (g) |
|------|--------------|---------------|---------|--------|--------------------|
| 1 | 31°02.080 | 103°28.118 | 50 | 0.132 | 0.889 |
| 2 | 31°00.597 | 103°28.016 | 86 | 0.064 | 0.794 |
| 3 | 31°00.032 | 103°32.855 | 100 | 0.028 | 0.590 |
| 4 | 31°01.338 | 103°33.196 | 40 | 0.094 | 0.635 |
| 5 | 31°01.344 | 103°33.177 | 18 | 0.157 | 0.636 |
| 6 | 30°58.419 | 103°27.556 | 55 | 0.088 | 0.691 |
| 7 | 31°02.780 | 103°28.893 | 80 | 0.092 | 0.899 |
| 8 | 31°02.480 | 103°28.593 | 15 | 0.241 | 0.893 |
| 9 | 31°02.180 | 103°28.111 | 30 | 0.177 | 0.897 |
| 10 | 31°01.750 | 103°28.131 | 15 | 0.229 | 0.865 |
| 11 | 31°01.441 | 103°28.197 | 36 | 0.142 | 0.840 |
| 12 | 30°58.876 | 103°27.435 | 43 | 0.108 | 0.719 |
| 13 | 31°00.173 | 103°27.605 | 11 | 0.246 | 0.787 |
| 14 | 31°00.528 | 103°28.084 | 8 | 0.275 | 0.787 |
| 15 | 31°00.120 | 103°27.491 | 36 | 0.138 | 0.789 |
| 16 | 30°59.444 | 103°26.416 | 8 | 0.269 | 0.795 |
| 17 | 30°59.467 | 103°26.580 | 36 | 0.138 | 0.789 |
| 18 | 30°59.282 | 103°27.696 | 5 | 0.293 | 0.731 |
| 19 | 30°58.996 | 103°27.651 | 32 | 0.134 | 0.718 |
| 20 | 30°59.106 | 103°28.425 | 45 | 0.105 | 0.694 |
| 21 | 31°00.412 | 103°30.119 | 16 | 0.183 | 0.698 |
| 22 | 30°59.448 | 103°26.737 | 30 | 0.149 | 0.781 |
| 23 | 30°58.980 | 103°27.527 | 23.7 | 0.155 | 0.721 |
| 24 | 31°00.578 | 103°30.625 | 17.3 | 0.167 | 0.688 |
| 25 | 31°01.584 | 103°30.768 | 6.4 | 0.27 | 0.735 |
| 26 | 31°00.054 | 103°27.471 | 15.3 | 0.195 | 0.785 |
| 27 | 30°59.944 | 103°27.371 | 10.8 | 0.244 | 0.783 |
| 28 | 30°59.448 | 103°26.737 | 18.4 | 0.193 | 0.781 |
| 29 | 30°58.984 | 103°27.563 | 26.4 | 0.135 | 0.720 |
| 30 | 30°58.735 | 103°27.500 | 50.2 | 0.095 | 0.709 |
| 31 | 30°58.814 | 103°27.679 | 29.1 | 0.134 | 0.707 |
| 32 | 30°58.296 | 103°27.531 | 13.6 | 0.191 | 0.686 |
| 33 | 30°58.031 | 103°27.502 | 71.4 | 0.073 | 0.674 |
| 34 | 30°59.204 | 103°28.648 | 21.2 | 0.157 | 0.691 |
| 35 | 30°59.438 | 103°28.970 | 11.5 | 0.209 | 0.691 |
| 36 | 30°59.673 | 103°29.065 | 19.5 | 0.16 | 0.699 |
| 37 | 31°00.365 | 103°30.306 | 8.3 | 0.225 | 0.689 |
| 38 | 31°00.619 | 103°31.669 | 29.7 | 0.125 | 0.653 |
| 39 | 31°00.657 | 103°31.731 | 12.4 | 0.177 | 0.653 |
| 40 | 31°00.795 | 103°32.115 | 10.6 | 0.196 | 0.646 |
| 41 | 31°00.868 | 103°32.393 | 88.5 | 0.058 | 0.640 |
| 42 | 31°01.866 | 103°32.555 | 29.3 | 0.126 | 0.682 |
| 43 | 31°01.900 | 103°32.697 | 7.2 | 0.241 | 0.679 |
| 44 | 31°01.056 | 103°32.874 | 10.2 | 0.198 | 0.633 |
| 45 | 31°01.172 | 103°33.004 | 32 | 0.108 | 0.634 |

Table 1 (continued)

| Nos. | Latitude (N) | Longitude (E) | DN (cm) | AC (g) | Calculated PGA (g) |
|------|--------------|---------------|---------|--------|--------------------|
| 46 | 31°01.380 | 103°33.274 | 13.1 | 0.191 | 0.635 |

Fig. 6 Comparison between predicted and measured values

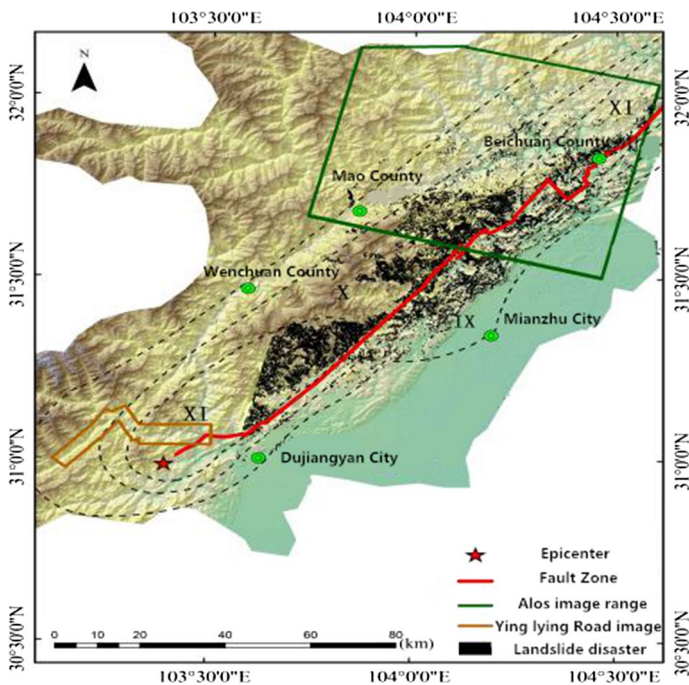
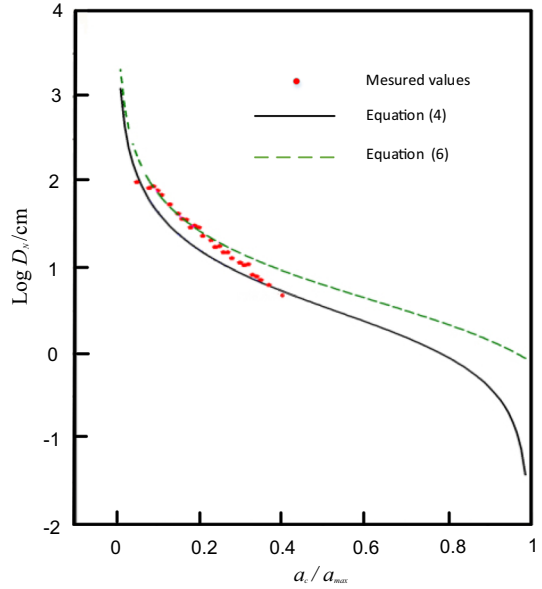


Fig. 7 Study area

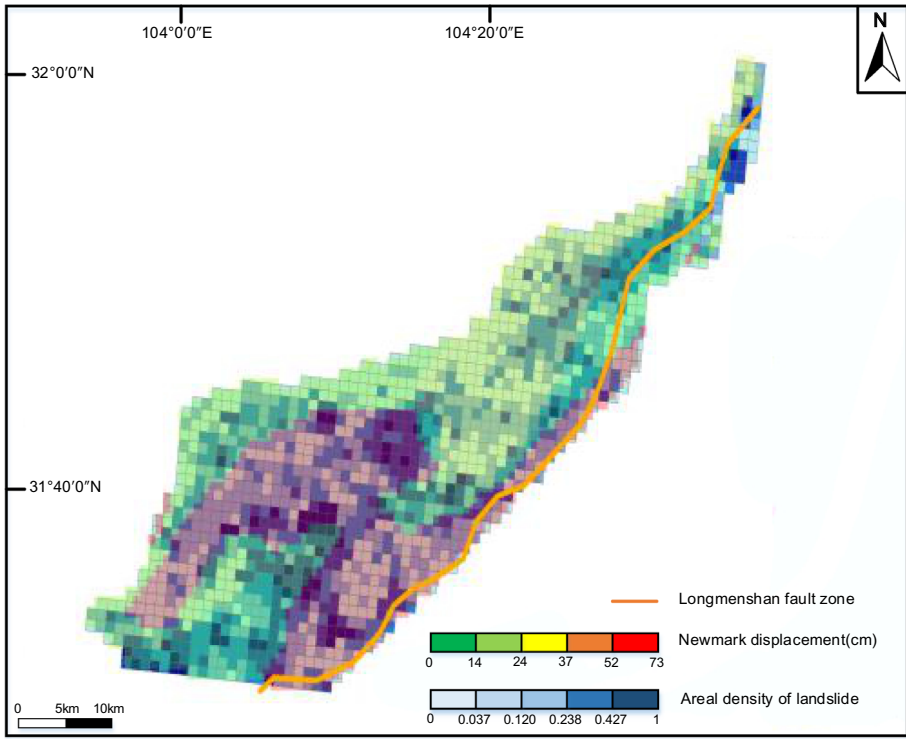


Fig. 8 Displacement and areal density data

Table 2 Newmark displacement calculation and landslide surface density

| Numbers | Displacement (cm) | Areal density (landslide area/ km ²) |
|---------|-------------------|--|
| 1 | 60.35 | 0.301 |
| 2 | 44.81 | 0.299 |
| 3 | 35.78 | 0.240 |
| 4 | 30.34 | 0.219 |
| 5 | 25.21 | 0.153 |
| 6 | 23.42 | 0.130 |
| 7 | 20.62 | 0.094 |
| 8 | 16.03 | 0.078 |
| 9 | 5.01 | 0.013 |
| 10 | 0 | 0 |

5.2 Study on hazard zoning for seismically triggered landslides

Based on the trend of the areal density curve, a criterion of classification with areal density as an index was proposed for earthquake-triggered landslide areas, as shown in Table 3.

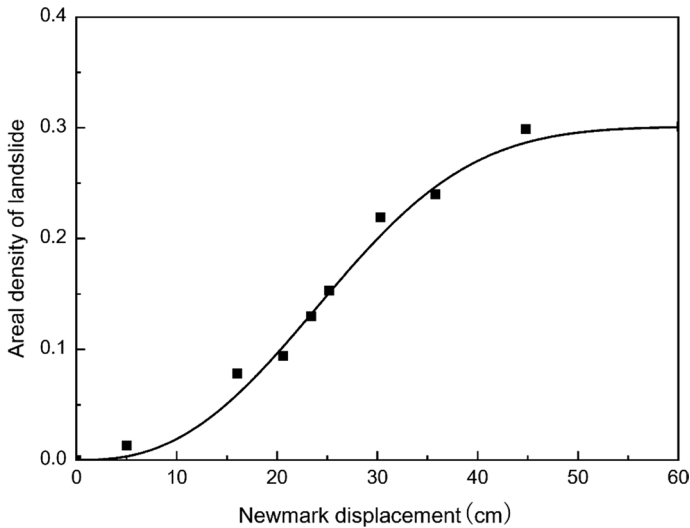


Fig. 9 Landslide density curve

On the basis of analyzing the trend of the areal density curve, we divided the severity of seismically triggered landslides into three levels: (1) mild danger zone: the displacement ranged from 0 to 10 cm (corresponding areal density of landslides: 0–0.03). No structural damage occurred on the slope, and the shear strength was approximately the same before the earthquake; (2) moderate danger zone: the displacement ranged from 10 to 40 cm (corresponding areal density of landslides: 0.03–0.27). Slopes suffered the structural damage, but there was still residual strength. Landslides were widely distributed; and (3) severe danger zone: the displacement value was more than 40 cm (corresponding areal density of landslides: 0.27–0.30). Slopes were prone to disintegration, and landslides were distributed densely.

5.3 Rationality verification of the hazard zoning method with the data of the Lushan earthquake

The Lushan earthquake presents an ideal case to test the accuracy of the hazard zoning method. The epicenter is located at 30°18'N, 103°E with the intensity of IX, and a depth of 13 km. The Lushan earthquake triggered more than 1600 landslides, which provides favorable conditions for the rationality test of hazard zoning method. The scope of the study area is from 30°10'0"N to 30°20'0"N latitudes and 102°50'0"E–103°10'0"E longitudes, covering an area of 422 km², and including part of the VIII-degree zone and the entire IX-degree zone.

In order to test the rationality of the risk zoning method, we compared the real distribution of the areal density of landslides in the study area with the predicted distribution. As mentioned before, the calculation of the modified Newmark displacements in the study area required two aspects of data: the information of a_c and the *PGA*. The shear strength parameters for a_c are shown in Table 4, and the *PGA* information can be obtained from the zoning map of ground-motion peak acceleration in China. The results showed that the

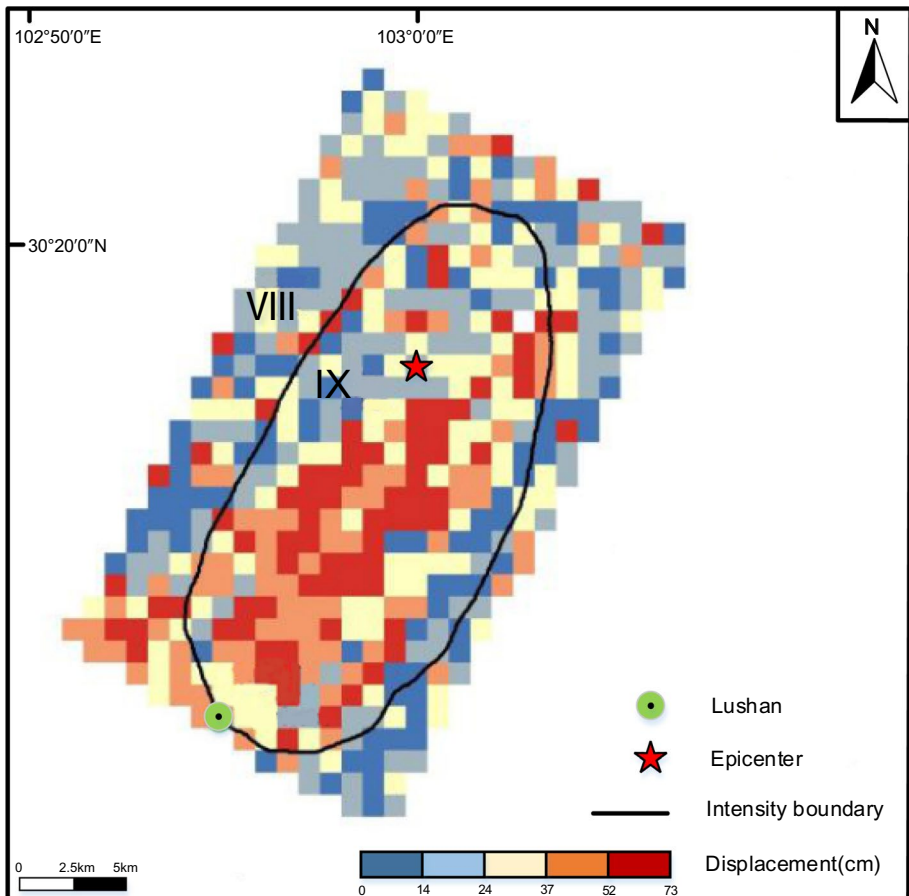
Table 3 Earthquake-triggered landslide hazard classification system

| Severity partition | Landslide density (landslide area/km ²) | Disaster severity description |
|---------------------------|---|---|
| I (Mild danger zone) | 0–0.03 | The co-seismic disaster is mainly caused by falling rock and partial and landslide; when the permanent displacement of the slope is less than 10 cm, the slope is damaged to a certain extent, but the strength can be maintained the same before the earthquake; the change in the formation conditions of the mountain disaster after the earthquake is not significant. Secondary disasters are mainly caused by the significant increase in rockfall. The secondary mountain disasters triggered by earthquake are not the major disaster that controls the route selection |
| II (Moderate danger zone) | 0.03–0.27 | During the earthquake, the distribution of landslides is wide, and there were not many large-scale mountain damages; the permanent displacement reached 10–40 cm, and the slope body suffered structural damage, but it remains residual strength; the mountain disaster is active after the earthquake; comparisons are supposed to be made between the pass plan and the avoidance plan by using risk analysis |
| III (Severe danger zone) | 0.27–0.30 | Earthquake and landslides are often densely distributed. When the permanent displacement reaches 40 cm or more, the slope body is prone to disintegration. After the earthquake, geological disasters occur frequently, and large-scale mountain disasters are prone to occur. The recovery period of geological environment is more than 10 years. The route selection design has to adopt a bypass scheme |

Table 4 Rock parameters in the study area

| Lithology | c' (MPa) | φ' (°) | Y (kN/m ³) | m | t (m) |
|-----------|------------|----------------|--------------------------|-----|---------|
| I | 0.027 | 35 | 25 | 1 | 5 |
| II | 0.020 | 20 | 22 | 1 | 5 |
| III | 0.015 | 10 | 15 | 1 | 5 |

Newmark displacements in study area ranged from 0 to 40 cm (Fig. 10). The displacements were 20–40 cm in the center of IX-degree zone; 20 cm or less at the junction of VIII and IX-degree zone; and less than 10 cm in the VIII-degree zone. On the basis of the displacements, the areal density of landslides in study area was obtained using Eq. 7. The study area was divided into two types of danger zone (the mild danger zone and the moderate danger zone) according to distribution of the areal density of landslides. The hazard zoning results and real earthquake-triggered landslides in the study area are both shown in Fig. 11. The average areal density of landslides was 0.013 in the mild danger zone and 0.21 in the

**Fig. 10** Prediction value of Newmark displacement

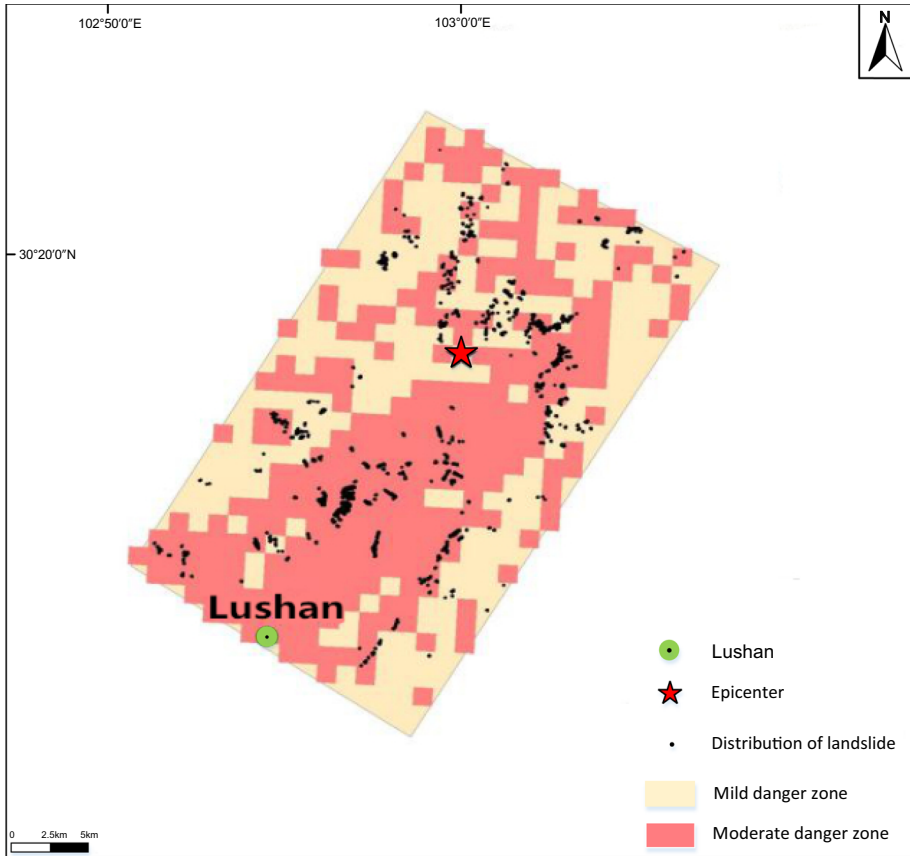


Fig. 11 Distribution of real landslide points of Lushan earthquake

moderate danger zone, respectively, which fell within the areal density interval of the hazard zoning method. Comparing with the phenomenon that more than 60% of the landslides in Lushan earthquake were concentrated in the very low hazard area in the traditional Newmark model calculated by Ma and Xu (2018), the hazard zoning method based on the modified Newmark model showed a good trend that the areal density of landslides increased rapidly with the increase in the hazard level. Therefore, the rationality of this seismic landslide hazard zoning method was verified using the data of the Lushan earthquake.

6 Conclusions

The Newmark model was modified by adding attenuation coefficients to the effective internal friction angle and cohesion (0.85 and 0.6, respectively), and the critical acceleration in this model is 0.7 times it before. The data of the Wenchuan earthquake showed that the accuracy of Jibson predicting method was significantly improved after the modification. Based on the modified Jibson method, a hazard zoning method for earthquake-triggered landslides with areal density as the zoning index was established. The severity of seismic

landslides was divided into three levels according to the areal density (mild danger zone: 0–0.03; moderate danger zone: 0.03–0.27; and severe danger zone: 0.27–0.3). The rationality of this hazard zoning method has been verified by the data of the Lushan earthquake. The hazard zoning method adopted the macroscopic index of areal density, which not only contains information on the deformation and damage of slopes, but also reflects the changes in the pregnancy environment of mountain disasters after the earthquake. Therefore, the hazard zoning method can provide a scientific basis for the construction of major projects in mountainous areas with a high seismic intensity.

Acknowledgements This study was supported by the National Natural Science Foundation of China (41530639 and 41571004).

References

- Al-Homoud AS, Tahtamoni W (2000) Comparison between predictions using different simplified Newmarks' block-on-plane models and field values of earthquake induced displacements. *Soil Dyn Earthq Eng* 19:73–90
- Ambraseys NN, Menu JM (1988) Earthquake-induced ground displacements. *Earthq Eng Struct Dyn* 16:985–1006
- Ambraseys NN, Srbulov M (1994) Attenuation of earthquake-induced displacements. *Earthq Eng Struct Dyn* 25:467–487
- Bray JD, Travasarou T (2007) Simplified procedure for estimating earthquake-induced deviatoric slope displacements. *J Geotech Geoenviron Eng* 133:381–392
- Chen QG, Ge H, Zhou HF (2011) Mapping of seismic triggered landslide through Newmark method: an example from study area Yingxiu. *Coal Geol China* 11:44–48 (in Chinese)
- Cui P, He SM, Yao LK (2011) Formation mechanism and risk control of mountain disaster in Wenchuan earthquake. The Science Publishing, Beijing, pp 102–103 (in Chinese)
- Decanini LD, Fabrizio M (2001) An energy-based methodology for the assessment of seismic demand. *Soil Dyn Earthq Eng* 21:113–137
- Duan SS, Yao LK, Guo CW (2015) Predominant direction and mechanism of landslides triggered by Lushan earthquake. *J Southwest Jiao Tong Univ* 3:428–434 (in Chinese)
- Gorum T, Fan XM, van Westen CJ, Huang RQ, Xu Q, Tang C, Wang GH (2011) Distribution pattern of earthquake-induced landslides triggered by the 12 May 2008 Wenchuan earthquake. *Geomorphology* 133(3–4):152–167
- Huang RQ, Li WL (2008) Research on development and distribution rules of geohazards induced by Wenchuan earthquake on 12th May, 2008. *Chin J Rock Mech Eng* 12:2585–2592 (in Chinese)
- Huang Y, Xiong M (2017) Dynamic reliability analysis of slopes based on the probability density evolution method. *Soil Dyn Earthq Eng* 94:1–6
- Huang Y, Hu HQ, Xiong M (2018) Probability density evolution method for seismic displacement-based assessment of earth retaining structures. *Eng Geol* 234:167–173
- Jaeger JC, Cook NGW (1969) *Fundamentals of rock mechanics*. Methuen and Company, London, p 513
- Jibson RW (1993) Predicting earthquake-induced landslide displacements using Newmark's sliding block analysis. *Transp Res Rec* 1411:9–17
- Jibson RW (2007) Regression models for estimating coseismic landslide displacement. *Eng Geol* 91:209–218
- Jibson RW, Keefer DK (1993) Analysis of the seismic origin of landslides: examples from the New Madrid seismic zone. *Geol Soc Am Bull* 105:521–536
- Jibson RW, Harp EL, Michael JA (2000) A method for producing digital probabilistic seismic landslide hazard maps. *Eng Geol* 58(3–4):271–289
- Keefer D (2000) Statistical analysis of an earthquake-induced landslide distribution: the 1989 Loma Prieta and California event. *Eng Geol* 58(3–4):231–249
- Keefer DK, Wilson RC (1989) Predicting earthquake-induced landslides, with emphasis on arid and semi-arid environments. *Landslides Semi Arid Environ* 2:118–149
- Khazai B, Sitar N (2000) Assessment of seismic slope stability using GIS modeling. *J Appl Physiol* 6:121–128

- Kokusho T, Ishizawa T (2006) Energy approach for earthquake induced slope failure evaluation. *Soil Dyn Earthq Eng* 26:221–230
- Kokusho T, Ishizawa T, Nishida K (2009) Travel distance of failed slopes during 2004 Chuetsu earthquake and its evaluation in terms of energy. *Soil Dyn Earthq Eng* 29:1159–1169
- Lee CT, Hsieh BS, Hsuan C (2012) Regional arias intensity attenuation relationship for Taiwan considering V_{s30} . *Bull Seismol Soc Am* 102:129–142
- Ling HI, Le D, Chou NS (2001) Post-earthquake investigation on several geosynthetic-reinforced soil retaining walls and slopes during the Ji–Ji earthquake of Taiwan. *Soil Dyn Earthq Eng* 21:297–313
- Ling HI, Liu H, Mohri Y (2005) Parametric Studies on the Behavior of Reinforced Soil Retaining Walls under Earthquake Loading. *J Eng Mech* 131(10):1056–1065
- Lveda SAS, Murphy AW, Jibson RW (2005) Seismically induced rock slope failures resulting from topographic amplification of strong ground motions: the case of Pacoima Canyon, California. *Eng Geol* 80:336–348
- Ma SY, Xu C (2018) Assessment of co-seismic landslide hazard using the Newmark model and statistical analyses: a case study of the 2013 Lushan, China, Mw6.6 earthquake. *Nat Hazards* 96:389–412. <https://doi.org/10.1007/s11069-018-3548-9>
- Milesa SB, Ho CL (1999) Rigorous landslide hazard zonation using Newmark's method and stochastic ground motion simulation. *Soil Dyn Earthq Eng* 18:305–323
- Newmark NM (1965) Effects of earthquakes on dams and embankments. *Geotechnique* 15:139–160
- Rajabi AM, Mahdavi MR, Khamehchiyan M, Gaudio VD (2011) A new empirical estimator of coseismic landslide displacement for Zagros Mountain region (Iran). *Nature Hazards* 59:1189–1203
- Rodriguez C, Bommer J, Chandler RJ (1999) Earthquake-induced landslides: 1980–1997. *Soil Dyn Earthq Eng* 18:325–346
- Rodríguez-Peças MJ, García-Mayordomo J, Azañón JM (2014) GIS application for regional assessment of seismically induced slope failures in the Sierra Nevada Range, South Spain, along the Padul fault. *Environ Earth Sci* 72:2423–2435
- Romeo R (2000) Seismically induced landslide displacements: a predictive mode. *Eng Geol* 58:337–351
- Shang YH, Lee CT (2011) Empirical estimation of the Newmark displacement from the Arias intensity and critical acceleration. *Eng Geol* 122:34–42
- Wang JC, Zao MJ, Chen W, Wang K (2012) Comparison of dynamic and static triaxial test on the soil-rock mediums. *Adv Mater Res* 446–449:1563–1567
- Wang T, Wu SR, Shi JS, Xing P (2013) Case study on rapid assessment of regional seismic landslide hazard based on simplified Newmark displacement model: Wenchuan as 8.0 earthquake. *J Eng Geol* 1:16–24 (in Chinese)
- Wieczorek GF, Wilson RC, Harp EL (1993) Map showing slope stability during earthquakes in San Mateo County, California. *Metall Mater Trans A* 681:155–164
- Wilson RC, Keefer DK (1985) Predicting areal limits of earthquake induced landsliding. *Geol Surv Prof Pap* 1360:317–345
- Xu C, Xu XW, Yao X, Dai FC (2014) Three (nearly) complete inventories of landslides triggered by the May 12, 2008 Wenchuan Mw 7.9 earthquake of China and their spatial distribution statistical analysis. *Landslides* 11(3):441–461
- Yin YP, Wang FW, Sun P (2009) Landslide hazards triggered by the 2008 Wenchuan earthquake, Sichuan, China. *Landslides* 6(2):139–152